

# Newly desertified regions in Iraq and its surrounding areas: Significant novel sources of global dust particles

Ali Moridnejad, Neamat Karimi, Parisa A. Ariya

## Abstract

Using the newly developed Middle East Dust Index (MEDI) applied to MODIS satellite data, we consider a relationship between the recent desertified regions, over the past three decades, and the dust source points identified during the period of 2001-2012. Results indicate that major source points are located in Iraq and Syria, and by implementing the spectral mixture analysis on the Landsat TM images (1984 and 2012), a novel desertification map was extracted. Results of this study indicate for the first time that *c.a.*, 39% of all detected source points are located in this newly anthropogenically desertified area. Using extracted indices for Deep Blue algorithm, dust sources were classified into three levels of intensity: low, medium, and high. A large number of low frequency sources are located within or close to the newly desertified areas. These severely desertified regions require immediate concern at a global scale.

## 1. Introduction

In recent decades, there has been increasing interest in understanding atmospheric physics and chemistry of aerosols, and aerosol-cloud interaction processes. Atmospheric aerosols are defined as condensed matter (liquid, solid or heterogeneous) suspended in the air. These aerosols consist of natural and anthropogenic species in particle form with aerodynamic diameters ranging from a few nm to several micrometers. The two ubiquitous and important natural kinds of aerosols are sea salt and mineral dust, which are emitted into the atmosphere as a result of wind stress at the ocean surface and arid land areas, respectively (Grini, 2004).

Aerosols and their interactions with clouds and radiation “contribute the largest uncertainty to the total radiative forcing estimate” affecting climate change. Dust aerosols can significantly impact the Earth's climate system (Mahowald et al., 2013; Choobari et al., 2014) by changing the radiation budget (Sokolik and Toon, 1996; Hansell et al., 2010, 2012; Valenzuela et al., 2012), cloud optical properties and lifetimes (Mahowald and Kiehl, 2003; Ou et al., 2012), and precipitation processes (Solomos et al., 2011; Creamean et al., 2013). They can also influence the Earth's ecosystems through marine and terrestrial biogeochemical cycles (Jickells et al., 2005; Mahowald et al., 2005; Okin et al., 2008), hydrologic processes (Painter et al., 2007; Neff et al., 2008) and human health (Griffin, 2007). Desertification, the damage to land that creates deserts, is a serious environmental threat for inhabitants of deserts and a main element of global change, causing wide scale land degradation in arid and semi arid regions of the world (Okin et al., 2009). Different forms of desertification take place in terms of patterns and processes. In this study, this term has been used to refer to the removal of vegetation and soil salinization and is driven by a number of social, political, economic, and natural factors (such as population growth, drought, climate variations or changes, tillage for cultivation and overgrazing). Indeed, vegetation cover and soil salinity (alone or combined) plays a major role in determining the biological composition of the soil and has been the main driver the development and increase in desertification. The concept of desertification and dust plumes is well incorporated. Such that, the term of desertification became well known in the 1930s when parts of the Great Plains in the United States turned into the Dust Bowl.

By studying the interactions between desertification and dust storms, scientists will be better able to understand the role human and natural induced factors play in the magnitude of dust storms (Ginoux et al., 2012; Rashki et al., 2013). Okin et al. (2001) in a study over the Mojave Desert found that abandoned agricultural fields can introduce deflationary surfaces by wind-transported materials into stable desert surfaces and can change their spectral reflectance (Okin and Painter, 2004). Additionally, wind-blown sand can lead to the expansion of desertification by burying, abrading, or stripping leaves from plants that are in the flow direction and potentially lengthen the pathway (Okin et al., 2009).

Human contribution to the mineral dust abundance has been estimated to be as high as 30-50 % (Sokolik and Toon, 1996; Tegen and Lacis, 1996). Some researchers have provided a sensitive link between desert dust emissions and climate; yet, how humans affect desert dust emissions is not well characterized (Mahowald et al., 2010), partly due to the fact that the anthropogenic forcing is very sensitive to models and meteorological conditions (Mahowald et al., 2002; Luo et al., 2003; Tegen et al., 2004).

The Middle East region has been considered to be responsible for approximately 25% of the Earth's global emissions of dust particles (Zender et al., 2003; Ginoux et al., 2004). This region, which has been experiencing severe environmental challenges is also most vulnerable to climate and human induced changes. Dust storms are one of the traditional outcomes of extreme weather events in arid and semi-arid countries located in this region and these have been more frequent and intense in the past decade (Karimi et al., 2012). Recent studies in the area have shown that Iraq and Syria are the major countries generating dust storms, noting that there is currently no consensus on the factors driving enhanced dust storms. Some contributing factors include inappropriate agricultural practices (UN SDS Report, 2013), unsustainable water resources management and climate change (Al-Ansari, 2013), military operations (Gibson, 2012) and land degradations (Sissakian et al., 2013). Gibson (2012) in a thorough study assessed whether cultivated areas in Iraq changed during or as a result of war and sanctions. The results indicate that cultivated areas changed little between the Iran-Iraq War (1980-1988) and the Gulf War (1990-1991), increased by 20 percent (from 1.72 to 2.04 Mha) during the period of the United Nations sanctions (1990-2003), and dropped to below pre-sanction levels (1.40 Mha) during Operation Iraqi Freedom (2003-2011). Also, more information on the impact of haphazard driving and military operations (thousands of trucks and heavy vehicles, explosion of numerous bombs and rockets) on

compacted top soil layers, causing emissions of dust, can be found in the work of Sissakian et al. (2013). These factors have been suggested as having major impacts on desertification in the region, and the increased challenges linked to regional dust storms. The aim of our study was to provide insights on the location, frequency and intensity of the new and mostly man-made dust storms. Also, the main objective of the present study is to determine the role of desertification in the process of the growing frequency and intensity of dust storms in the Middle East region. We herein concurrently deploy: (a) satellite data (NASA/MODIS and NASA Landsat TM), (b) dust source point identification techniques (using the newly developed Middle East Dust index to map the region); (c) spectral mixture analysis (for further desertification information extraction), and (d) change vector analysis (to study intensity of desertification change in the Middle East).

### **1.1. Background of study region**

The Middle East, which consists largely of the Arabian Plateau and the Tigris-Euphrates Basin, is one of the world's active wind erosion regions (Shao, 2008). The Arabian Plateau is generally considered to be from the southwest high terrains (1500-3000 m) bordering the Red Sea towards the northeast flat lands (50-200 m) next to the Persian Gulf (Idso, 1976) identified as Arabia, one of five world regions where dust storm generation is intense (Fig. 1). The area of desert, which stretches across Iraq, Iran, Afghanistan, Pakistan, and northwest India, has long been recognized as a source of atmospheric mineral dust (Bryson and Baerreis, 1967; Grigoryev and Kondratyev, 1981). The major southern interior of the Arabian Peninsula is made up of the Rub Al-Khali (or Empty Quarter, 582750 km<sup>2</sup>), which is one of the largest sand deserts in the world and is connected to the An Nafud sand sea in the north by the Ad Dahna (a sand corridor 1287 km long) (Shao, 2008).

Previously, researchers have recognized two major dust regions in the Middle East: (1) In 1986, Middleton carried out a preliminary analysis of the distribution and seasonality of dust storms using meteorological data and demonstrated that the Lower Meso-potamian plains (Iraq and Kuwait) exhibited the highest number of dust storm days per year (especially from April to August). Central Saudi Arabia showed a moderate level of dust storm. Note that previous studies have indicated the alluvial plains (Safar, 1980), off the Omani coast (Tindale and Pease, 1999) and Arabian Sea (Prospero and Carlson, 1981) have a considerable number of dust storms in the Middle East.

There are four dominant climate systems in the Middle East: (1) in winter, the Siberian anticyclone over central Asia; (2) the Polar anticyclone over east of Europe and the Mediterranean Sea, in the summer; (3) the monsoon cyclones over the Indian Subcontinent, the south and southeast of Iran and southeast of the Arabian peninsula, in the summer; (4) the depressions traveling from north of Africa and south and east of the Mediterranean sea across the Middle East and southwest of Asia in the non-summer seasons (spring and winter) (Hamidi et al., 2013). Two winds in particular generate dust in the region: The Shamal wind, which blows from mid-June to mid-September, creates severe summer Shamal dust storms, and prefrontal and postfrontal winds which generate frontal dust storms in other seasons (Wilkerson, 1991).

## **2. Data and methodology**

### **2.1. NASA/MODIS**

Moderate Resolution Imaging Spectroradiometer (MODIS) data were used to compare several dust retrieval algorithms and to apply a new approach to identify dust source points by a combination of the visible (VIS) and thermal infrared (TIR) bands. This sensor makes observations using 36 bands with wavelengths ranging from 0.41 to 14.4  $\mu$ m and nadir spatial resolution of 0.25, 0.5, and 1 km. MODIS, launched in December 1999 and May 2002, respectively, is operating onboard the NASA Earth Observing System (EOS) Terra and Aqua satellites. MODIS data were obtained from the Level 1 Atmosphere Archived and Distribution System and processed to convert the digital numbers into radiometrically calibrated and geo-located data products. The daily MODIS Level 2 Aerosol data were also used. These data are produced at spatial resolutions of about 1  $\times$  1 km pixel arrays.

### **2.2. NASA/Landsat TM**

The Landsat Thematic Mapper (TM) sensor was carried onboard Landsats 4 and 5 from July 1982 to May 2012 with a 16-day repeat cycle. Images consist of seven spectral bands with a spatial resolution of 30 m for Bands 1 to 5 and 7. Spatial resolution for Band 6 (thermal infrared) is 120 m. This data was used in change detection analysis and desertification extraction. Since we are looking for the trend and potential impact of desertification on the dust source point developments, the study tried to define a possible longer period of time for better analysis. On the other hand, the availability of data and the highest number of cloud-free images giving almost a full coverage for the region within a year were other factors in choosing the time domain. We used data from the Landsat TM sensor that has been operational since 1984. Therefore, 1984 and 2011 were selected as the boundaries of the study. According to our hydrologic analysis, both years are normal rainfall years as well.

Therefore, 32 cloud and dust free satellite images, of equal scale, were used and analyzed. More importantly, based on the goal of this study and other similar studies for land and water cover change detection, the date of the images is obtained at the end of the growing season. Consequently, all images were acquired for September, which is considered the end of the growing season in the Middle East region.

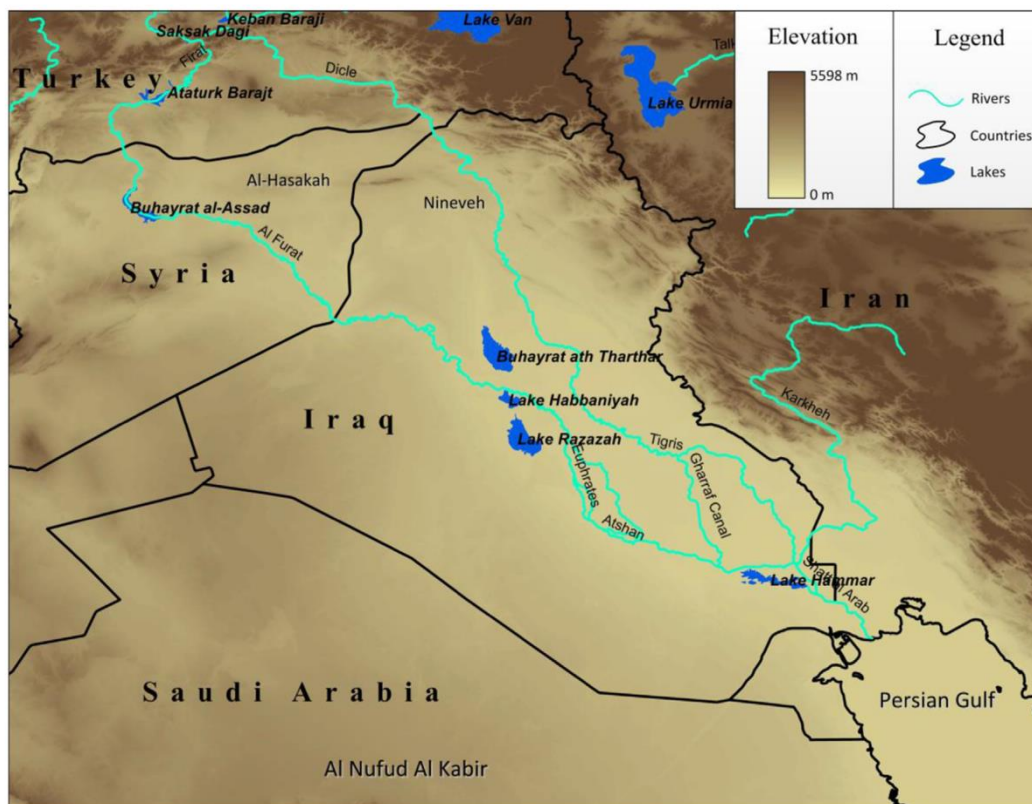


Fig. 1. Iraq and its surrounding countries (Background image shows the topography of study area).

### 2.3. Source point identification

We used satellite observations to illustrate a new mapping technique for dust source points in the Middle East region to retrieve spatial pattern, area, and intensity of each source point and to interpret different countries' contributions to the generation of dust storms in the study area. Unlike ocean and water surfaces, it is very difficult to detect mineral aerosol (or dust events) over the surface of desert and land bodies due to the similar reflectivity of mineral aerosol and desert lands using unadjusted VIS satellite imagery. In addition, several challenges (such as sensor capability and model accuracy) exist in differentiating mineral aerosol from cloud, sea salt, and anthropogenic pollution. As a result, a number of studies have used brightness temperature changes between mineral aerosols and land surfaces to distinguish them from each other (Ackerman, 1989; Miller, 2003). The use of single TIR has had limited success due to the changes in surface emissivity (Roskovensky and Liou, 2003, 2005). Because of this limitation as well as the emissive variability and the transmissive properties of mineral particles within multi-TIR ranges, several algorithms have been invented based on the brightness temperature difference (BTD), as bi-spectral split window techniques. BTD is based on temperature differences between the ground surface and cooler mineral aerosols while at the same time are largely unaffected by absorption from other atmospheric gases (Darmenov and Sokolik, 2005).

The dust source identification method in this study is based on the new model, called Middle East Dust Index (MEDI) retrieved in the previous work by Karimi et al. (2012). In MEDI, four major dust source identification models: (Ackerman's model, Roskovensky and Liou algorithm, Normalized Difference Dust Index (NDDI), Deep Blue algorithm) were analyzed and compared within the study region, and the advantages and shortcomings were evaluated. To analyze the performance of different MODIS dust retrieval methods in identifying source points, three dust events, which originated in the Middle East region, were studied. Because of the specific situation of the Middle East area (more brilliant desert, mineralogical diversity of source points, and dust storm occurrence in different meteorological conditions), these techniques could not effectively differentiate dust plume from the bright desert surfaces (due to the same thermal behavior of dust and desert surfaces in both BT31 and BT32). Consequently, we previously strived to develop a new approach by gathering all points to improve dust plume identification using MODIS data called MEDI. In this model, BT29 was involved to highlight the

difference between dust and desert surfaces. Several factors, which can significantly affect dust plume and source identification, have also been included in MEDI, namely single or multiple dust plumes and multi-mineralogical dust plumes. In addition to the satellite-based algorithms, the HYbrid Single-Particle Lagrangian Integrated Trajectory (HYSPPLIT) model was used to recognize dust sources in each event separately. For dust source identification, we first developed a new model, MEDI, specifically designed for the Middle East region, and then applied it to all MODIS images associated with 70 dust storms occurring in the period 2001 to 2012.

$$MEDI = \left[ \frac{(BT_{31} - BT_{29})}{(BT_{32} - BT_{29})} \right] \times A \quad (1)$$

$$A = -999 \text{ if } NDDI < 0 \\ A = 1 \text{ if } NDDI > 0 \quad (2)$$

$$NDDI = \frac{\rho_{2.13} - \rho_{0.469}}{\rho_{2.13} + \rho_{0.469}} \quad (3)$$

$$Dust = MEDI < 0.6 \quad (4)$$

Where BT is the brightness temperature in MODIS bands,  $\rho$  is the reflectance of dust. Normalized Difference Dust Index (NDDI) is another dust characterization factor, which enables the MEDI model to better distinguish dust plumes in the satellite images.

After validation of MEDI and ensuring that it is capable of dust source identification, this model was applied, in this study, to 70 separate storms during the period of 2001 and 2012.

Although our new model shows its capability to determine dusty pixels more accurately, some mismatches of our models should be noted here. First, in the case of cirrus clouds, some misidentifications were found and the NDDI index was used to modify them. Also, in snow-covered areas, some misclassifications were detected in some cases. This can introduce some errors in winter storms and in the high mountain areas of Iran as most of the time these regions are snow covered. Thus, it is suggested that before using the MEDI model, the Normalized Difference Snow Index (NDSI) should be used to eliminate the snow-covered areas. Although in MEDI the 0.6 threshold value (dust B 0.6) can identify dusty pixels sufficiently, it should be adjusted for each event separately using its relevant histogram, because like other discriminating algorithms, this value can vary based on the thermal properties of ground surface and the amount of moisture content.

#### 2.4. Desertification extraction

Vegetation indexes (such as Normalized Difference Vegetation Indexes (NDVI)) and image classification approaches (including maximum-likelihood, clustering and discrimination analysis) have been most commonly used to map spatial and temporal variation in vegetation covers and ultimately desertification monitoring (Tucker, 1979; Dawelbait and Morari, 2012). But the biggest obstacle and difficulty of these methods is the existence of mixed pixels in the satellite imagery used. This issue is more common in using low and medium spatial resolution satellite images (e.g., Landsat-TM and MODIS images). Therefore, if the aforementioned techniques (vegetation indexes and classification approaches) are used for desertification monitoring, to obtain an accurate measurement, the pixel size of the image used must be smaller than the scale of variability of at least one of the principle landscape elements (e.g., trees or grasslands). One of the best and most efficient solutions to resolve this problem is to use sub-pixel classification techniques that could be used to unmix the soil-plant canopy measurements into the respective soil, vegetation, and non-photosynthetic vegetation. In other words, one approach for measuring desertification in terms of the relative proportion of vegetation covers in image pixels is the Spectral Mixture Analysis (SMA) method that can quantify the proportion of each pixel occupied by individual image components.

In order to study desertification, several factors prompted the use of the SMA in the present study: (1) Sparser vegetation cover due to the arid and semi-arid characteristics of the study area; (2) Inefficiency of the common classification methods; (3) Higher accuracy of the spectral mixture analysis method compared to vegetation indices approaches; (4) The ability of the spectral mixture analysis method to identify the intensity and direction of changes over land at the same time.

Implementation of SMA techniques consists of three steps: (A) identification and assessment of the dominant phenomena in a landscape for endmember selection, (B) identification of end-members within a pixel and extraction of their spectral libraries, (C) determine the contribution of each of the dominant phenomena (endmembers) in each pixel of satellite image used. SMA can be implemented in different ways, whereby the Linear SMA (LSMA) is the most common and most popular. The basic LSMA equation is as follows (Okin and Robert, 2004; Dawelbait and Morari, 2012):

$$R_p(\lambda) = \sum_{i=1}^n f_i R_i(\lambda) + \varepsilon(\lambda)$$

Where  $R_p(\lambda)$  is the surface reflectance of each individual pixel,  $f_i$  is the weighting coefficient (the sum of all values will be equal

to one) and interpreted as a fraction of each pixel made up of endmember (e.g., soil, vegetation of salt),  $R_i(\lambda)$  is the amount of reflectance for each endmember in a n-endmember model and  $\varepsilon(\lambda)$  is the difference between the actual and modeled reflectance.

Endmembers selection is the most critical step in SMA (Tompkins et al., 1997). Although there are many approaches for selecting endmembers (e.g., image endmember and library end- member), image endmember selection based on the Principle Component Analysis (PCA) approach is more common and has been used frequently for change detection analysis (Elmore et al., 2000; Bateson and Curtiss, 1996; Bateson et al., 2000). Two advantages of this technique are that the selection of the endmember spectra is based on the inherent spectral variability of the image data without requiring homogeneous pixels of each endmember and its simple implementation (Asner, 2004; Dawelbait and Morari, 2012). A more detailed description of image endmember selection is given by Dawelbait and Morari (2012).

After implementing the spectral mixture analysis, trend of changes for four main extracted features including soil, vegetation, salt, and water covers were analyzed over Iraq and Syria which, between 1984 and 2011, were two major source points of severe and frequent dust storms in the Middle East region. Since the study area is very large (c.a., 547,000 km<sup>2</sup>), it was divided into two separate upper and lower parts and 16 Landsat-TM images were merged in order to obtain the complete coverage of the area.

### 2.5. Change Vector Analysis (CVA)

Although trend of changes for different covers was done separately, it is not possible to have a comprehensive analysis of all parameters together. In fact, these types of comparisons can specifically explain changes in different covers; however they do not interpret the possibility of identifying the desertified regions and making final decisions for dust storm source points. Consequently, besides these comparisons, changes were analyzed using the CVA method. Euclidean distance was used to measure the intensity of changes. To identify the direction of changes, change vector was employed as a function of angle in each satellite image in time 1 (1984) and time 2 (2012). Three dimensional vector analyses were used, in which trend of changes for three parameters, which included soil, vegetation, and salt covers were analyzed at the same time. By implementing this model, two major types of changes were observed. The first is the new irrigated farmlands as a result of agricultural development along the rivers and irrigation networks in the region and the second type of changes is the area in which the vegetation, soil, and salt covers have been degraded toward being a desert. As previously mentioned, this category mainly includes the abandoned farmlands no longer used for agriculture and farming. Fig. 2 contains a flowchart outlining how the desertification map is extracted.

## 3. Results and discussion

By studying all the dust sources points in the Middle East in the period from 2001 to 2012, it was found that major dust spots are located in Iraq and Syria when compared to the other countries of the region. Our results indicate that approximately 12,218 km<sup>2</sup> of both Iraq and Syria has become desertified during the past three decades (Fig. 3). Note these areas have recently joined traditional sources of dust storms in the region such as the Saudi Arabian deserts, which now significantly incorporates dust emissions. The major desertified areas identified through change detection analysis are located between the Euphrates and Tigris Rivers which include northeastern Syria and northwestern and western parts of Iraq (elevation 270-640 m), some parts of central and eastern Iraq close to the border of Iran (elevation 3-360 m), and finally the northern border of Saudi Arabia with Iraq and Jordan (elevation 790-930 m). Lakes were separately classified into two groups: dried and generated. In addition to desertification, an increase in the vegetation cover (regrowth) was also detected and was categorized into low and high regrowth.

As depicted in Fig. 3, the highest area of concentration for severe desertification is located in the northwestern border of Iraq and Syria from Nineveh in Iraq to Al-Hasakah in Syria. This region predominantly comprises farmlands, and is close to the border of Turkey. The topography and river morphology of this region indicates that constructed dams and water control in river basins have significantly reduced the stream flow, which impacts the downstream zones. Another large portion of both high and low intensity desertified areas originates in the northern part of the Euphrates River between Tharthar Lake in Iraq and the Iraq-Syria border and continues through scattered areas in central and eastern parts of Iraq.

A large number of low desertified zones were found in the lowlands (elevation between 20 and 25 m), along the Euphrates River before and after the city of Najafol Ashraf. Interestingly enough, the highest concentration of high and low regrowth lands is also located in this zone. The main reason for this consequence is that most parts of this area, which was already desertified, have recently been recovered by releasing the stream flow in the up- stream (Richardson et al., 2005).

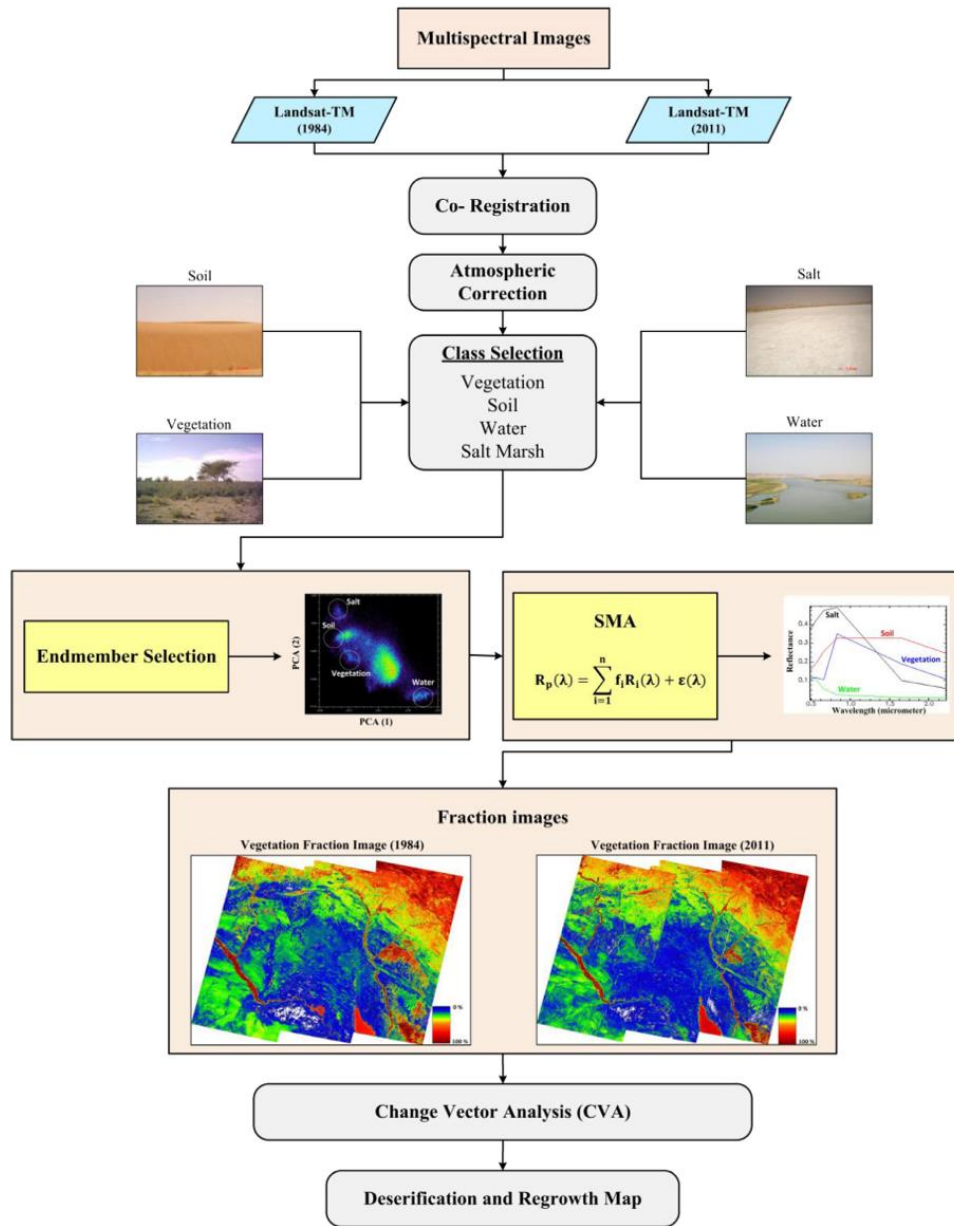


Fig. 2. Spectral Mixture Analysis procedure for delineating desertified areas.

Our results (Fig. 3) show that Rezazza Lake in northeastern Karbala in the heart of Iraq has severely shrunk to less than half the size, compared to three decades ago. The Euphrates River is the source of water for this lake as well as for Habbaniyah Lake to the north of Rezazza Lake. The surface area of Tharthar Lake, located in northwestern Baghdad, which is fed by the Tigris River, has also decreased in both sides and in the north. In the last decade, several small bodies of water, close to Nineveh and in the eastern parts of Iraq, have been completely desiccated (Fig. 3).

Water surface has increased by about 550 km<sup>2</sup> (Table 1) in the sites of the newly constructed dams' reservoirs that impound large lakes including Mosul Dam Lake, Dukan Lake, Haditha Dam Lake and Al-Azim Dam Lake in Iraq and Ad Dughayrat Dam Lake in Syria. Growth change analysis (Table 1), indicates that the highest regrowth areas are mostly located along the rivers and downstream of the newly-constructed regional dam. The main factor for the increase in green lands surface is attributed to the

agricultural development and the establishment of irrigation systems and harvesting water from the rivers. Such changes are observed in northeastern and eastern Syria along the Euphrates River especially from Deir z-Zur to Al Bukamal and north of Al Hasakah. Kirkuk, in Iraq, can be considered a regrowth focal point along with other regions in northwestern Iraq up to Diyala in the East and Najafol Ashraf, Al Qadesiyyah, Dhi Qar, Wasit and Maysan in central and eastern Iraq. These areas are mostly marshlands and wetlands that have recently been recovered (Richardson et al., 2005).

The extracted desertification map was superimposed on to the identified atmospheric dust source points in the Middle East region on the basis of recently developed Middle East Dust Index (MEDI) applied to 70 dust storms, which occurred in the period between 2001 and 2012 (Fig. 4). Results indicate that about 39% of the 243 different identified source areas, which participated in generating dust storms, are located in the newly desertified regions. Although there are desertified regions in the lower half of Iraq, the concentration and the total area of dust source points increases, up from the center of Iraq to the north and northwest as well as to the north and northeast Syria. These regions also contain the highest concentration of desertified areas and dried lakes, suggesting a positive relationship between desertification and dust source points.

There are other areas in eastern Syria, bordering Jordan with Iraq and Saudi Arabia, mid south and eastern parts of Iraq close to the border of Iran, that source points are not well overlaid on the desertification areas. Several factors can explain this observation. Firstly, there are a number of source points in the study area that are already located in existing deserts and our model shows that the venue of these sources has not changed during the last 30 years. Secondly, there are new desertified regions that experienced changes including loss of vegetation cover, desiccation, or land degradation; however, they do not appear to be source points for generating dust storms, yet, they can potentially become future dust source points. Of major concern is the fact that a large portion of desertified regions is unevenly distributed in distinct climate zones, across several countries, which traditionally do not cooperate, thereby making it difficult for environmental scientists and policy makers, to efficiently overcome obstacles or implement further preventative actions to protect the lands and bodies of water, or control and manage the magnitude and rate of changes.

Since throughout the year, one specific, large area source point may not necessarily play a significant role in dust storm emissions, all the identified dust source points during a 12 year period were carefully analyzed on the basis of their frequency of occurrence and intensity. Results of this analysis show that the area of a source point is proportional to its frequency of occurrence. One of the important parameters considered in this study is dust source point classification based on intensity. Using extracted indices for Deep Blue algorithm, identified dust sources are classified into three levels in terms of intensity: low, medium, and high. The desertification map was superimposed on the frequency (Fig. 4A) and intensity (Fig. 4B-D) of dust source points. Of note is that a large number of low frequency sources are located within or close to the newly desertified areas (Fig. 4A). Sources of higher intensity and frequency are also located in northwestern Iraq and in eastern Syria, where a large portion of the land has recently been desertified.

We classified recent alterations in desertification patterns in the study zone into three main categories. The first group belongs to those agricultural lands, abandoned by farmers during the last decades, which are now barren lands. These changes can be observed in northern parts of Iraq, near the Syrian border, and in eastern parts of Syria. Major causes of these land use changes in Iraq are due to drought, consecutive wars, and the lack of available water resources. The importance of dust emissions in these areas is that 40 out of the 243 source areas identified during the past 12 years are located in these abandoned agricultural fields, and thus the new desertification is predominantly anthropogenically driven. About 49% of all dust events, occur in these regions, exhibiting the highest intensity. The second type of changes is in relation to the lakes and wetlands, which have dried out and have been affected by a decrease in the amount of river flow mainly due to constructed dams on the main river or through drought. However, they have not significantly participated in generating dust storms and only few source points can be found in the dry lake margins. The third type of desertification in Iraq and Syria is in relation to the semi-desert and desert regions, which have been affected in terms of their vegetation cover and/or land condition. This category of changes is the dominant type of changes in the region and is the most important phenomenon responsible for increases in dust storms during recent years.

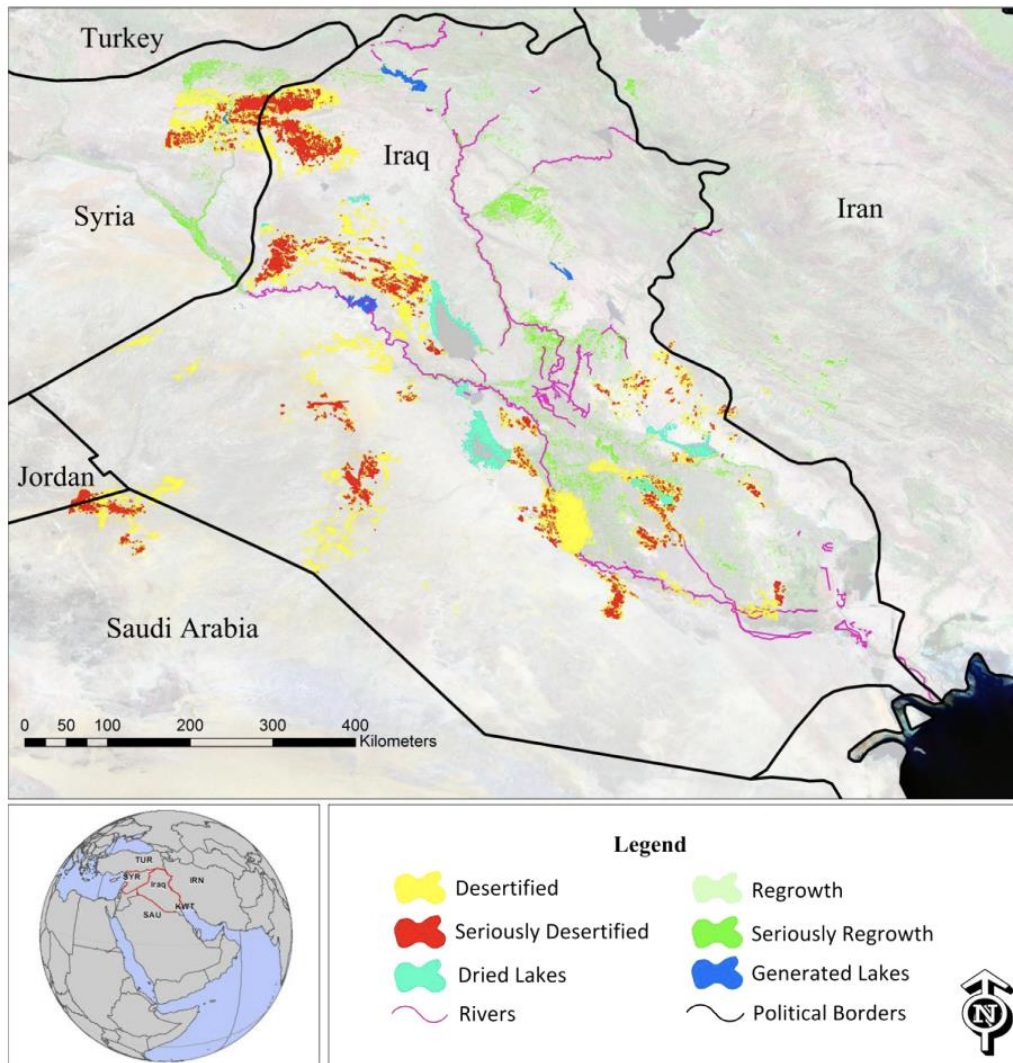


Fig. 3. The newly desertified regions over Middle East region involved in dust storm.

**Table 1**  
 Area of different desertified categories in Iraq and Syria.<sup>a</sup>

Desertified- high (km <sup>2</sup> )	Desertified- low (km <sup>2</sup> )	Dried water (km <sup>2</sup> )	Regrowth water (km <sup>2</sup> )	Regrowth low (km <sup>2</sup> )	Regrowth High (km <sup>2</sup> )
6968	3752	1498	550	1191	2512

<sup>a</sup> The cumulative error is less than or equal to  $\pm 5$  percent.

#### 4. Conclusion

Based on AOD<sub>550 nm</sub> analysis (derived from MODIS-Terra satellite image) it was revealed that the amount of AOD has increased since 2001. Mean daily AOD over Iraq and its surrounding area increased from 0.28 in 2001 to about 0.4 in 2013 (red line in Fig. 5). Also, the number of days with AOD greater than 0.3 increased dramatically during last 13 years (black line in Fig. 5). The AOD greater than 0.3 was used because this threshold usually indicates days whereby dust storms happen in the Middle East. Fig. 5 indicates that the mean daily AOD >0.3 increased from 0.45 since 2001 to about 0.53 in 2013. Due to the dramatic recent increase in the number of dust storms, it can be concluded that significant portions of these new desertified regions are the additional causes of generating dust events, which have not been seen in the past. Fig. 6, shows one of the new dust plumes which were derived from desertified areas. Notwithstanding that most current source points were also active in the past, proper measures have yet to be taken to control their emissions. Although we did not detect significant changes over these old desert sources in the past three decades, they have produced a considerable amount of dust in the region and according to satellite images, have also emitted to neighboring countries. Indeed, in the Middle East, during the past 12 years, *c.a.* 28% of all dust events (*c.a.*, 100) initiated at known dust emission sources. In total, approximately 39% of all analyzed dust events (144 out of 367 events) generated in areas, which have been desertified over the past three decades. In other words, these new emission sources form a significant portion of the global dust storms source points. Dust aerosols have wide ranging complex physical and chemical properties that can also undergo atmospheric (photo) chemical aging and cloud nucleation processes.

The Middle East is a high petroleum-producing hub, which generates substantial waste in air, water and soil, and thus the produced dust particles may have added chemical composition complexity as well as physical and radiative properties. Further integrated research (measurement and observation, laboratory and modeling) is needed to evaluate the local, regional and global impact of these new and mostly anthropogenic sources of dust aerosols on human health, air quality, extreme weather, hydro- logical cycle, radiation,

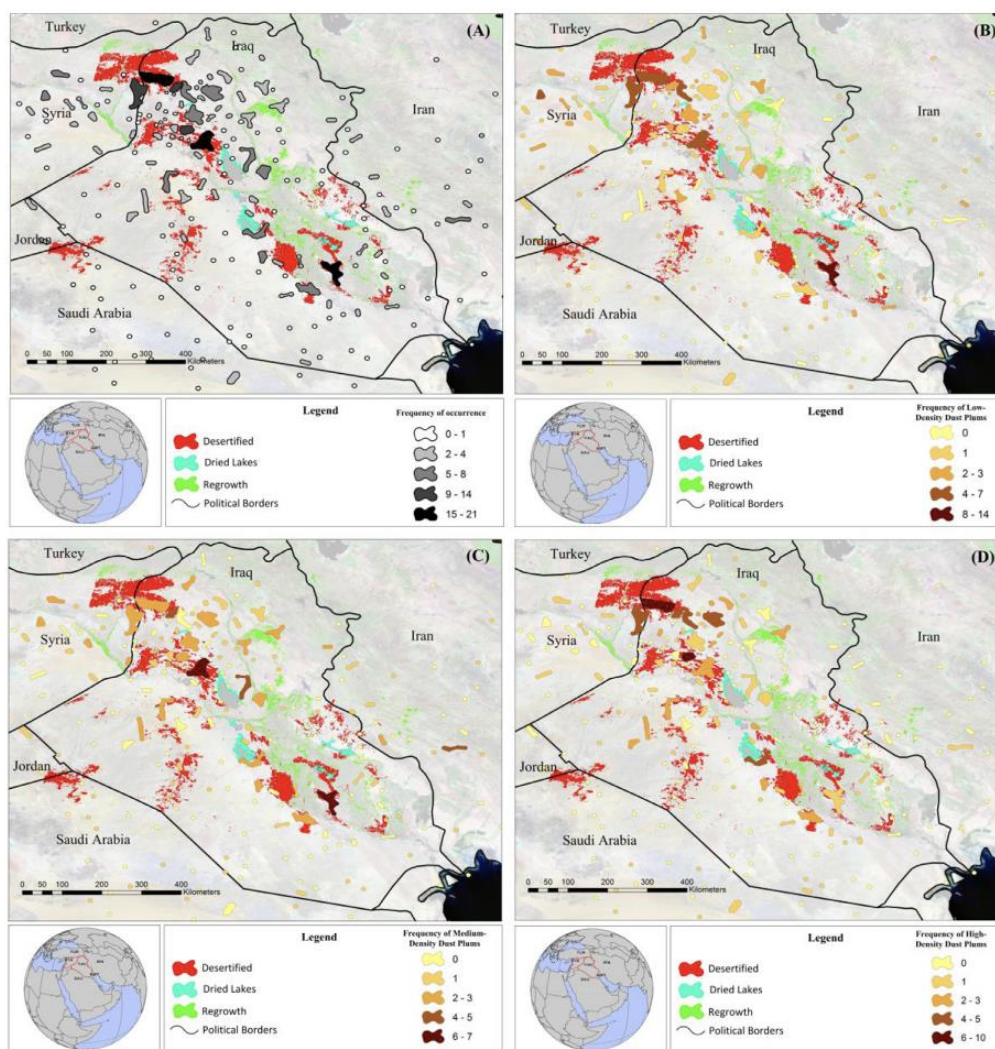


**Fig. 4.** Schematic of the Middle East region involved in dust storm generation; (A) Dust storms' frequency of occurrence; (B) map of the low intensity dust source points; (C) map of the medium intensity dust source points; (D) map of the high intensity dust source points.

cloud physics and Earth's biogeochemical cycles. Further international collaboration is also required in order to transfer knowledge into action towards the remediation and prevention of additional drastic desertification.

## Acknowledgment

We acknowledge the financial support of these Canadian funding agencies: Natural Sciences and Engineering Research Council of Canada (223464), fonds de recherche du Québec: Nature et technologies, and Canadian Foundation for Innovation. Data for this study are available at NASA LANCE Rapid Response (MODIS MYD04\_L2 product), NASA GIOVANNI Data and Information Services Center (Deep Blue and AOD products), USGS Earth Explorer (SRTM data and Landsat TM images), NOAA Physical Science Division (NCEP/NCAR Reanalysis product for wind direction), NOAA Air Resource Laboratory (HYSPLIT back trajectory for source point evaluation), and Google Earth images over study area. We thank Dr. P. Ginoux who generously sent us the original data used for comparative work in this study.

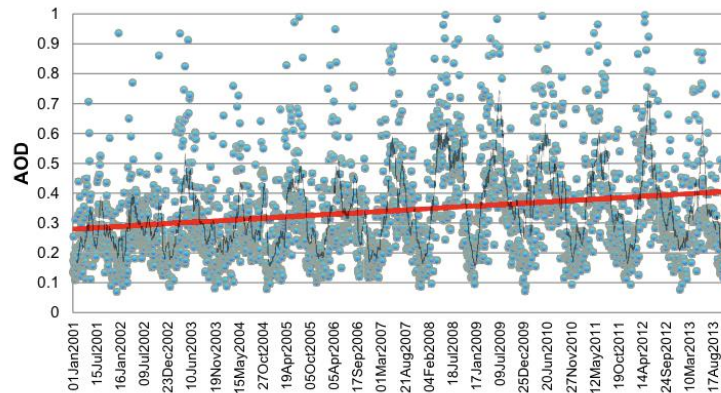


**Fig. 5.** Daily mean variation and linear regression trends (red line) for the area-averaged MODIS-Aerosol Optical Depth (AOD550) in Iraq during the period 2001–2013. Black line indicates the trend of AOD > 0.3. (For interpretation of the references to colour in this figure legend, the reader is referred to the web version of this article.)

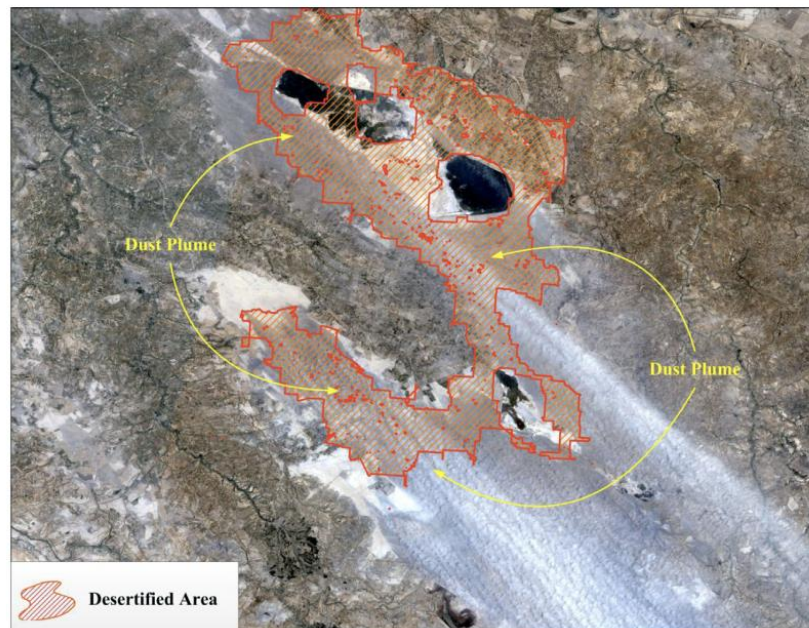


**Fig. 6.** Dust plumes occurring from a desertified area. Background image is a Landsat-TM satellite image acquired in May 2012.

## References

Ackerman, S.A., 1989. Using the radiative temperature difference at 3.7 and 11  $\mu\text{m}$  to track dust outbreaks. *Remote. Sens.*

© This manuscript version is made available under the CC-BY-NC-ND 4.0 license

<https://creativecommons.org/licenses/by-nc-nd/4.0/>

<https://www.sciencedirect.com/science/article/pii/S0140196315000099>

Environ. 27, 129e133. [http://dx.doi.org/10.1016/0034-4257\(89\)90012-6](http://dx.doi.org/10.1016/0034-4257(89)90012-6).

Al-Ansari, N.A., 2013. Management of water resources in Iraq: perspectives and prognoses. *Engineering* 5, 667e684. <http://dx.doi.org/10.4236/eng.2013.58080>. Asner, G.P., 2004. Biophysical remote sensing signatures of arid and semiarid ecosystem. In: Ustin, S.L. (Ed.), *Remote Sensing for Natural Resources Management and Environmental Monitoring*, third ed. Hoboken, New Jersey, pp. 53e109.

Bateson, C.A., Asner, G.P., Wessman, C.A., 2000. Endmember bundles: a new approach to incorporating endmember variability in spectral mixture analysis. *IEEE Trans. Geosci. Remote Sens.* 38, 1083e1094. <http://dx.doi.org/10.1109/36.841987>.

Bateson, C.A., Curtiss, B., 1996. A method for manual endmember selection and spectral unmixing. *Remote Sens. Environ.* 55, 229e243. [http://dx.doi.org/10.1016/S0034-4257\(95\)00177-8](http://dx.doi.org/10.1016/S0034-4257(95)00177-8).

Bryson, R.A., Baerreis, D.A., 1967. Possibilities of major climatic modification and their implications, Northwest India: a case for study. *Am. Meteorol. Soc. Bull.* 48, 136e142.

Choobari, O.A., Zawar-Reza, P., Sturman, A., 2014. The global distribution of mineral dust and its impacts on the climate system: a review. *Atmos. Res.* 138, 152e165. <http://dx.doi.org/10.1016/j.atmosres.2013.11.007>.

Creamean, J.M., Suski, K.J., Rosenfeld, D., Cazorla, A., DeMott, P.J., Sullivan, R.C., White, A.B., et al., 2013. Dust and biological aerosols from the Sahara and Asia influence precipitation in the Western US. *Science* 339, 1572e1578. <http://dx.doi.org/10.1126/science.1227279>.

Darmenov, A., Sokolik, I.N., 2005. Identifying the regional thermal IR radiative signature of mineral dust with MODIS. *Geophys. Res. Lett.* 32, L16803. <http://dx.doi.org/10.1029/2005GL023092>.

Dawelbait, M., Morari, F., 2012. Monitoring desertification in a Savannah region in Sudan using landsat images and spectral mixture analysis. *J. Arid Environ.* 80, 45e55. <http://dx.doi.org/10.1016/j.jaridenv.2011.12.011>.

Elmore, A.J., Mustard, J.F., Manning, S.J., Lobell, D.B., 2000. Quantifying vegetation change in semiarid environments. *Remote Sens. Environ.* 73, 87e102. <http://dx.doi.org/10.3410/f.1087903.540845>.

Gibson, G.R., 2012. *War and Agriculture: Three Decades of Agricultural Land Use and Land Cover Change in Iraq*. Virginia Polytechnic Institute and State University. Diss.

Ginoux, P., Prospero, J.M., Torres, O., Chin, M., 2004. Long-term simulation of global dust distribution with the GOCART model: correlation with North Atlantic Oscillation. *Environ. Model. Softw.* 19, 113e128. [http://dx.doi.org/10.1016/S1364-8152\(03\)00114-2](http://dx.doi.org/10.1016/S1364-8152(03)00114-2).

Ginoux, P., Prospero, J.M., Gill, T.E., Hsu, N.C., Zhao, M., 2012. Global-scale attribution of anthropogenic and natural dust sources and their emission rates based on MODIS Deep Blue aerosol products. *Rev. Geophys.* 50, RG3005. <http://dx.doi.org/10.1029/2012RG000388>.

Griffin, D.W., 2007. Atmospheric movement of microorganisms in clouds of desert dust and implications for human health. *Clin. Microbiol. Rev.* 20, 459e477. <http://dx.doi.org/10.1128/CMR.00039-06>.

Grigoryev, A.A., Kondratyev, K.J., 1981. Atmospheric dust observed from space. Part2. *WMO Bull.* 30, 3e9.

Grini, A., 2004. *Natural Aerosols in the Global Atmosphere*. Univ. of Oslo, Norway. PhD Dissertation, Dep. of Geos.

Hamidi, M., Kavianpour, M.R., Shao, Y., 2013. Synoptic analysis of dust storms in the Middle East. *Asia Pac. J. Atmos. Sci.* 49, 279e286.

Hansell, R.A., et al., 2012. An assessment of the surface longwave direct radiative effect of airborne dust in Zhangye, China, during the Asian Monsoon Years field experiment (2008). *J. Geophys. Res.* 117, D00K39. <http://dx.doi.org/10.1029/2011JD017370>.

Hansell, R.A., Tsay, S.C., Ji, Q., Hsu, N.C., Jeong, M.J., Wang, S.H., Reid, J.S., Liou, K.N., Ou, S.C., 2010. An assessment of the surface longwave direct radiative effect of airborne Saharan dust during the NAMMA field campaign. *J. Atmos. Sci.* 67, 1048e1065. <http://dx.doi.org/10.1175/2009JAS3257.1>.

Idso, S.B., 1976. Dust storms. *Sci. Am.* 235 (4), 108e11, 113e14.

Jickells, T.D., An, Z.S., Andersen, K.K., Baker, A.R., Bergametti, G., Brooks, N., Cao, J.J., et al., 2005. Global iron connections between desert dust, ocean biogeochemistry, and climate. *Science* 308, 67e71. <http://dx.doi.org/10.1126/science.1105959>.

© This manuscript version is made available under the CC-BY-NC-ND 4.0 license

<https://creativecommons.org/licenses/by-nc-nd/4.0/>

<https://www.sciencedirect.com/science/article/pii/S0140196315000099>

Karimi, N., Moridnejad, A., Golian, S., Samani, J.M.V., Karimi, D., Javadi, S., 2012. Comparison of dust source identification techniques over land in the Middle East region using MODIS data. *Can. J. Remote Sens.* 38, 586e599. <http://dx.doi.org/10.5589/m12-048>.

Luo, C., Mahowald, N., Corral, J., 2003. Sensitivity study of meteorological parameters on mineral aerosol mobilization, transport and distribution. *J. Geophys. Res.* 108, 4447, 4410.1029/2003JD0003483.

Mahowald, N., Albani, S., Kok, J.F., Engelstaeder, S., Scanza, R., Ward, D.S., Flanner, M.G., 2013. The size distribution of desert dust aerosols and its impact on the Earth system. *Aeolian Res.* <http://dx.doi.org/10.1016/j.aeolia.2013.09.002> (in press).

Mahowald, N., Kiehl, L., 2003. Mineral aerosol and cloud interactions. *Geophys. Res. Lett.* 30 (9), 1475., <http://dx.doi.org/10.1029/2002GL016762>.

Mahowald, N.M., Baker, A.R., Bergametti, G., Brooks, N., Duce, R.A., Jickells, T.D., Kubilay, N., Prospero, J.M., Tegen, I., 2005. Atmospheric global dust cycle and iron inputs to the ocean. *Glob. Biogeochem. Cycles* 19, GB4025. <http://dx.doi.org/10.1029/2004GB002402>.

Mahowald, N.M., Kloster, S., Engelstaedter, S., Moore, J.K., Mukhopadhyay, S., McConnell, J.R., Albani, S., Doney, S.C., Bhattacharya, A., Curran, M.A.J., Flanner, M.G., Hoffman, F.M., Lawrence, D.M., Lindsay, K., Mayewski, P.A., Neff, J., Rothenberg, D., Thomas, E., Thornton, P.E., Zender, C.S., 2010. Observed 20th century desert dust variability: impact on climate and biogeochemistry. *Atmos. Chem. Phys.* 10, 10875e10893. <http://dx.doi.org/10.5194/acp-10-10875-2010>.

Mahowald, N.M., Zender, C.S., Luo, Savoie, D., Torres, O., del Corral, J., 2002. Understanding the 30-year Barbados desert dust record. *J. Geophys. Res.* 107 (D21), 4561., <http://dx.doi.org/10.1029/2002JD002097>.

Middleton, N.J., 1986. Dust storms in the Middle East. *J. Arid Environ.* 10, 83e96.

Miller, S.D., 2003. A consolidated technique for enhancing desert dust storms with MODIS. *Geophys. Res. Lett.* 30 (20), 2071. <http://dx.doi.org/10.1029/2003GL018279>.

Neff, J.C., Ballantyne, A.P., Farmer, G.L., Mahowald, N.M., Conroy, J.L., Landry, C.C., Overpeck, J.T., Painter, T.H., Lawrence, C.R., Reynolds, R.L., 2008. Increasing eolian dust deposition in the western United States linked to human activity.

*Nat. Geosci.* 1, 189e195. <http://dx.doi.org/10.1038/ngeo133>.

Okin, G.S., Mladenov, N., Wang, L., Cassel, D., Caylor, K.K., Ringrose, S., Macko, S.A., 2008. Spatial patterns of soil nutrients in two southern African savannas. *J. Geophys. Res.* 113, G02011. <http://dx.doi.org/10.1029/2007JG000584>.

Okin, G.S., Murray, B., Schlesinger, W.H., 2001. Degradation of sandy arid shrubland environments: observations, process modelling, and management implications. *J. Arid Environ.* 47, 123e144. <http://dx.doi.org/10.1006/jare.2000.0711>.

Okin, G.S., Painter, T.H., 2004. Effect of grain size on remotely sensed spectral reflectance of sandy desert surfaces. *Remote Sens. Environ.* 89 (3), 272e280. <http://dx.doi.org/10.1016/j.rse.2003.10.008>.

Okin, G.S., Parsons, A.J., Wainwright, J., Herrick, J.E., Bestelmeyer, B.T., Peters, D.C., Fredrickson, E.L., 2009. Do changes in connectivity explain desertification? *BioScience* 59 (3), 237e244. <http://dx.doi.org/10.1525/bio.2009.59.3.8>.

Okin, G.S., Robert, D.A., 2004. Remote sensing in arid regions: challenges and opportunities. In: Ustin, S.L. (Ed.), *Remote Sensing for Natural Resources Management and Environmental Monitoring*, third ed. Hoboken, New Jersey, pp. 111e145.

Ou, S.C., Liou, K.N., Hsu, N.C., Tsay, S.C., 2012. Satellite remote sensing of dust aerosol indirect effects on cloud formation over Eastern Asia. *Int. J. Remote Sens.* 33, 7257e7272. <http://dx.doi.org/10.1038/nature01091>.

Painter, T.H., Barrett, A.P., Landry, C.C., Neff, J.C., Cassidy, M.P., Lawrence, C.R., McBride, K.E., Farmer, G.L., 2007. Impact of disturbed desert soils on duration of mountain snow cover. *Geophys. Res. Lett.* 34, L12502. <http://dx.doi.org/10.1029/2007GL030284>.

Prospero, J.M., Carlson, T.N., 1981. Saharan air outbreaks over the tropical North Atlantic. *Pure Appl. Geophys.* 119 (3), 677e691. <http://dx.doi.org/10.1007/BF00878167>.

Rashki, A., Kaskaoutis, D.G., Goudie, A.S., Kahn, R.A., 2013. Dryness of ephemeral lakes and consequences for dust activity: the case of the Hamoun drainage basin, southeastern Iran. *Sci. Total. Environ.* 463, 552e564. <http://dx.doi.org/>

© This manuscript version is made available under the CC-BY-NC-ND 4.0 license

<https://creativecommons.org/licenses/by-nc-nd/4.0/>

<https://www.sciencedirect.com/science/article/pii/S0140196315000099>

10.1016/j.scitotenv.2013.06.045.

Richardson, C.J., Reiss, P., Hussain, N.A., Alwash, A.J., Pool, D.J., 2005. The restoration potential of the Mesopotamian marshes of Iraq. *Science* 307, 1307e1311. [http:// dx.doi.org/10.1126/science.1105750](http://dx.doi.org/10.1126/science.1105750).

Roskovensky, J.K., Liou, K.N., 2003. Detection of thin cirrus from 1.38 mm/0.65 mm reflectance ratio combined with 8.611 mm brightness temperature difference. *Geophys. Res. Lett.* 30 (19) <http://dx.doi.org/10.1029/2003GL018135>.

Roskovensky, J.K., Liou, K.N., 2005. Differentiating airborne dust from cirrus clouds using MODIS data. *Geophys. Res. Lett.* 32, L12809. <http://dx.doi.org/10.1029/2005GL022798>.

Safar, M.I., 1980. Frequency of Dust in Day Time Summer in Kuwait. Directorate of Civil Aviation, Meteorological Dept., Climatological Section, State of Kuwait, pp. 107e119.

Shao, Y., 2008. Physics and Modelling of Wind Erosion. In: *Atmos. Oceanographic Sci. Lib. Ser.*, vol. 37. Springer, Heidelberg, Germany.

Sissakian, V., Al-Ansari, N., Knutsson, S., 2013. Sand and dust storm events in Iraq. *Nat. Sci.* 5, 1084e1094. <http://dx.doi.org/10.4236/ns.2013.510133>.

Sokolik, I.N., Toon, O.B., 1996. Direct radiative forcing by anthropogenic airborne mineral aerosols. *Nature* 381, 681e683. <http://dx.doi.org/10.1038/381681a0>.

Solomos, S., Kallos, G., Kushta, J., Astitha, M., Tremback, C., Nenes, A., Levin, Z., 2011. An integrated modeling study on the effects of mineral dust and sea salt particles on clouds and precipitation. *Atmos. Chem. Phys.* 11, 873e892. [http:// dx.doi.org/10.5194/acp-11-873-2011](http://dx.doi.org/10.5194/acp-11-873-2011).

Tegen, I., Lacis, A.A., 1996. Modeling of particle size distribution and its influence on the radiative properties of mineral dust aerosol. *J. Geophys. Res.* 101, 19237e19244. <http://dx.doi.org/10.1029/95JD03610>.

Tegen, I., Werner, M., Harrison, S.P., Kohfeld, K.E., 2004. Relative importance of climate and land use in determining present and future global soil dust emission. *Geophys. Res. Lett.* 31, L05105. <http://dx.doi.org/10.1029/2003GL019216>.

Tindale, N.W., Pease, P.P., 1999. Aerosols over the Arabian Sea: atmospheric transport pathways and concentrations of dust and sea salt. *Deep Sea Res. II* 46, 1577e1595. [http://dx.doi.org/10.1016/S0967-0645\(99\)00036-3](http://dx.doi.org/10.1016/S0967-0645(99)00036-3).

Tompkins, S., Mustard, J.F., Pieters, C.M., Forsyth, D.W., 1997. Optimization of end-members for spectral mixture analysis. *Remote. Sens. Environ.* 59, 472e489. [http://dx.doi.org/10.1016/S0034-4257\(96\)00122-8](http://dx.doi.org/10.1016/S0034-4257(96)00122-8).

Tucker, C.J., 1979. Red and photographic infrared linear combinations for monitoring vegetation. *Remote Sens. Environ.* 8 (2), 127e150. [http://dx.doi.org/10.1016/0034-4257\(79\)90013-0](http://dx.doi.org/10.1016/0034-4257(79)90013-0). UN Sand and Dust Storm Fact Sheet, 2013. <http://reliefweb.int/report/iraq/sand-and-dust-storm-fact-sheet>.

Valenzuela, A., Olmo, F.J., Lyamani, H., Antón, M., Quirantes, A., Alados-Arboledas, L., 2012. Aerosol radiative forcing during African desert dust events (2005e2010) over Southeastern Spain. *Atmos. Chem. Phys. Discuss.* 12, 6593e6622. [http:// dx.doi.org/10.5194/acp-12-10331-2012](http://dx.doi.org/10.5194/acp-12-10331-2012).

Wilkerson, W.D., 1991. Dust and Sand Forecasting in Iraq and Adjoining Countries. Air Weather Service, Scott AFB (AWS/XTX), Illinois, USA. Tech. Rep., 62225e5008.

Zender, C.S., Bian, H., Newman, D., 2003. Mineral Dust Entrainment and Deposition (DEAD) model: description and 1990s dust climatology. *J. Geophys. Res.* 108, 4416. <http://dx.doi.org/10.1029/2002JD002775>, D14.